

Dopant-Free GaN/AlN/AlGa_N Radial Nanowire Heterostructures as High Electron Mobility Transistors

Yat Li,[†] Jie Xiang,[†] Fang Qian,[†] Silviya Gradečak,[†] Yue Wu,[†] Hao Yan,[†]
Douglas A. Blom,[§] and Charles M. Lieber^{*,†,‡}

*Department of Chemistry and Chemical Biology, Harvard University,
Cambridge, Massachusetts 02138, Division of Engineering and Applied Science,
Harvard University, Cambridge, Massachusetts 02138, and Metals and Ceramics
Division, Oak Ridge National Laboratory, Oak Ridge, Tennessee 37831*

Received April 14, 2006

ABSTRACT

We report the rational synthesis of dopant-free GaN/AlN/AlGa_N radial nanowire heterostructures and their implementation as high electron mobility transistors (HEMTs). The radial nanowire heterostructures were prepared by sequential shell growth immediately following nanowire elongation using metal–organic chemical vapor deposition (MOCVD). Transmission electron microscopy (TEM) studies reveal that the GaN/AlN/AlGa_N radial nanowire heterostructures are dislocation-free single crystals. In addition, the thicknesses and compositions of the individual AlN and AlGa_N shells were unambiguously identified using cross-sectional high-angle annular darkfield scanning transmission electron microscopy (HAADF-STEM). Transport measurements carried out on GaN/AlN/AlGa_N and GaN nanowires prepared using similar conditions demonstrate the existence of electron gas in the undoped GaN/AlN/AlGa_N nanowire heterostructures and also yield an intrinsic electron mobility of 3100 cm²/Vs and 21 000 cm²/Vs at room temperature and 5 K, respectively, for the heterostructure. Field-effect transistors fabricated with ZrO₂ dielectrics and metal top gates showed excellent gate coupling with near ideal subthreshold slopes of 68 mV/dec, an on/off current ratio of 10⁷, and scaled on-current and transconductance values of 500 mA/mm and 420 mS/mm. The ability to control synthetically the electronic properties of nanowires using band structure design in III-nitride radial nanowire heterostructures opens up new opportunities for nanoelectronics and provides a new platform to study the physics of low-dimensional electron gases.

Semiconductor nanowires^{1,2} are attractive building blocks for nanoscale electronic devices, including field-effect transistors (FETs),^{3–5} inverters,⁶ logic circuits,⁷ and decoders,⁸ because of the intrinsic small size and promise of enhanced mobility from 1D confinement effects. Yet, continued progress toward integrated nanoelectronic circuits will require advances in our ability to better control the electronic properties of these building blocks and to assemble them into increasingly complex structures. Considerable efforts have been placed on doping in Si,^{4,6,8b} Ge,⁵ and GaN^{9,10} nanowires to control their electrical properties. Despite this progress, doping of nanostructures remains a challenge¹¹ as a result of both fundamental synthetic issues and statistical fluctuations that are intrinsic to homogeneous doping of small structures. Moreover, charged dopant centers can limit mobilities and the corresponding performance of semiconductor materials in general.¹²

To overcome these issues, we have been exploring the potential of band structure engineering by creating radial

nanowire heterostructures.^{13–15} This work has been motivated by studies of undoped and delta-doped planar heterostructures that have been shown to form two-dimensional electron and hole gases, which have served as key platforms for both fundamental studies and high-speed electronic applications.¹² Such heterostructures can exhibit high carrier mobility due to a reduction or elimination of impurity scattering by separating the dopants and surface potential fluctuations from the conduction channel. We have recently demonstrated a one-dimensional (1D) hole gas in undoped Ge/Si core/shell radial nanowire heterostructures^{14,15} and, moreover, shown that these nanowires have potential as high-performance p-type FETs.¹⁵ It is important to understand the potential generality of this approach for creating nanowire carrier gases because both electron and hole gases are needed (i) to enable high-performance complementary nanoelectronics, which can increase switching speeds with low power consumption versus unipolar devices, and (ii) to explore and compare the fundamental properties of both 1D electron and hole gases. Here we report a rational synthesis of undoped GaN/AlN/AlGa_N radial nanowire heterostructures showing spontaneous formation of an electron gas and the application of these nanowire heterostructures as HEMTs.

* Corresponding author. E-mail: cml@cmliris.harvard.edu.

[†] Department of Chemistry and Chemical Biology, Harvard University.

[‡] Division of Engineering and Applied Science, Harvard University.

[§] Metals and Ceramics Division, Oak Ridge National Laboratory.

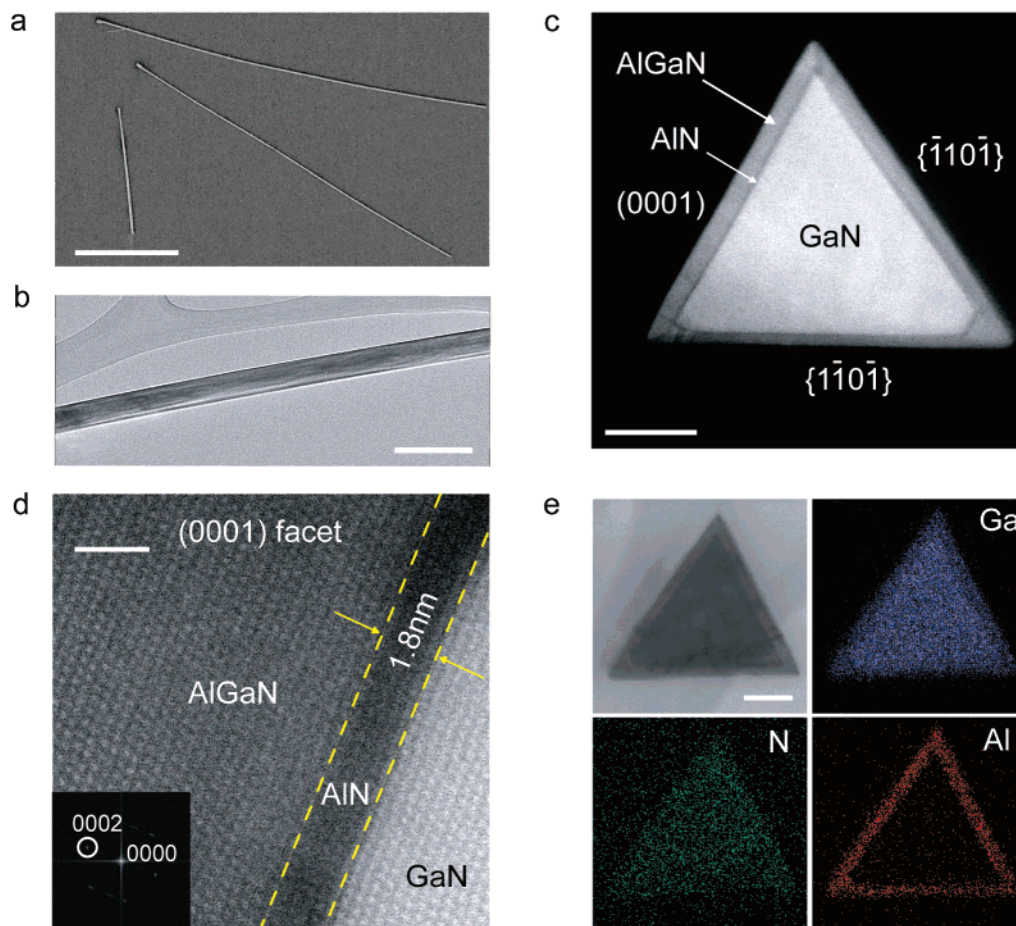


Figure 1. (a) SEM image of GaN/AlN/AlGaIn nanowires on a substrate. Scale bar is 5 μm . (b) Bright-field low-resolution TEM image of a GaN/AlN/AlGaIn nanowire. Scale bar is 500 nm. (c) HAADF-STEM image of a GaN/AlN/AlGaIn nanowire cross section. Scale bar is 50 nm. (d) Lattice-resolved HAADF-STEM image recorded at the (0001) facet of the nanowire. Dashed lines highlight the heterointerfaces between layers. Scale bar is 2 nm. Inset: electron diffraction pattern indexed for the [11-20] zone axis. (e) Bright-field STEM image and the corresponding EDX elemental mapping of the same nanowire, indicating spatial distribution of Ga (blue), Al (red), and N (green), recorded on a GaN/AlN/AlGaIn nanowire cross section. Scale bar is 50 nm.

Our designed nanowire structure consists of an intrinsic, high-purity GaN core and sequentially deposited undoped AlN and AlGaIn shells. In this structure, the GaN conduction band lies below that of AlGaIn, and because of the large internal electric field across the radial heterojunction between the GaN core and AlN/AlGaIn shells, which is due to strong spontaneous and piezoelectric polarization,¹⁶ an electron gas can form in the GaN. A thin epitaxial AlN interlayer (2 nm) was used in our design to reduce alloy scattering from the AlGaIn outer shell¹⁷ and to provide a larger conduction band discontinuity for better confinement of electrons. The thickness of the AlN layer is critical and must be below the estimated critical thickness obtained in the AlN planar structure (~ 3 nm)¹⁸ to prevent the introduction of dislocations or other defects that could lead to substantial carrier scattering. Previous studies reported that a GaN/AlGaIn radial nanowire structure could be formed spontaneously during MOCVD growth with Ga and Al precursors;¹⁹ although the required precise control of both the shell thickness and composition for our designed heterostructure precludes the use of such spontaneous processes.

To enable full control of the composition of the GaN nanowire core and compositions and thicknesses of the AlN/

AlGaIn shells during synthesis of the target GaN/AlN/AlGaIn radial nanowire heterostructures, we extended MOCVD methods described recently for the growth of GaN/InGaIn core/multishell light-emitting diodes.^{9,10,20} A scanning electron microscopy (SEM) image (Figure 1a) of as-prepared GaN/AlN/AlGaIn nanowires shows that the wires are uniform in diameter with typical nanowire lengths, which depend on the initial GaN core growth time, of 10–20 μm . Conventional TEM analysis of these nanowires revealed that they are single-crystal structures with a $\langle 11-20 \rangle$ growth direction. A representative low-resolution TEM image (Figure 1b) demonstrates that the nanowire is dislocation-free, as observed in all of the nanowires in our study. Dislocations are electron-trapping centers that could limit electron mobility;²¹ therefore, the absence of dislocations in these nanowires is important to our goal of making high-mobility electron gases. We note that the absence of dislocations is an advantage of our nanowire system; that is, contrary to planar growth, nanowire synthesis is effectively substrate-free, which prevents the formation of dislocations due to lattice mismatch between GaN and typical growth substrates.

In addition, cross-sectional TEM studies²² were carried out to visualize directly and to quantify the thickness and

chemical composition of the individual shells in GaN/AlN/AlGaIn nanowire heterostructures. A cross-sectional HAADF-STEM image (Figure 1c) of a representative GaN/AlN/AlGaIn nanowire taken along the $[11\bar{2}0]$ zone axis shows that the nanowire has a triangular cross section that consists of a (0001) facet and two crystallographically identical $\{-110\bar{1}\}$ planes, which is in agreement with our previous studies.^{9,10,23} The HAADF-STEM image shows strong contrast that is sensitive to the atomic number of the imaged materials.²⁴ The dark contrast region refers to the material with the smaller atomic number that gives less elastically scattered electrons, and in our case, is an AlN middle layer. Consequently, the outer shell and inner core could be assigned to be AlGaIn and GaN, respectively, consistent with our targeted structure. A lattice-resolved HAADF-STEM image (Figure 1d) reveals that the heterointerfaces between the GaN core and the AlN/AlGaIn shells are atomically sharp, without boundary defects. This confirms the epitaxial deposition of AlN/AlGaIn shells and the absence of strain relaxation and suggests that scattering due to surface roughness should be reduced in these nanowire heterostructures. On the basis of the clear contrast, the thicknesses of the AlN and AlGaIn layers are estimated to be 1.8 and 10.2 nm, respectively. STEM energy-dispersive X-ray spectroscopy (EDX) elemental mapping (Figure 1e) of the GaN/AlN/AlGaIn nanowire cross section reveals clearly the spatial distribution of Ga, Al, and N in the structure, confirming that the contrasts in Figure 1c and d originate from the variation of chemical composition. On the basis of the EDX data recorded at the nanowire edge, the Al composition in the AlGaIn layer is estimated to be $25 \pm 1.5\%$, consistent with the growth conditions. Taken together, the HAADF-STEM and EDX studies confirm the successful growth of a GaN/AlN/Al_{0.25}Ga_{0.75}N nanowire with a well-defined thickness and composition.

Systematic transport measurements²⁵ were carried out to evaluate the electrical properties of FETs fabricated from the GaN/AlN/Al_{0.25}Ga_{0.75}N nanowires. Figure 2a shows the current (I_{ds}) versus drain-source voltage (V_{ds}) data recorded on a representative GaN/AlN/Al_{0.25}Ga_{0.75}N nanowire with a diameter of 100 nm (blue line). The nanowire device exhibits substantial current at zero gate voltage (V_{gs}), and the current first rises and then begins to saturate at more positive values of V_{ds} similar to an n-type metal oxide semiconductor field-effect transistor (MOSFET).¹² In addition, the $I_{ds} - V_{gs}$ data (Figure 2b, blue line) recorded on the same nanowire reveal that the nanowire current increases as V_{gs} becomes more positive, with a large peak transconductance (g_m) of ca. 2.4 μ S at $V_{ds} = 1$ V. These data demonstrate that the nanowire device behaves as n-type depletion mode FET¹² and confirm the accumulation of electron carriers. Control experiments were also carried out on undoped GaN nanowires prepared using the same growth conditions and having diameters similar to those of the GaN core in the heterostructures. Contrary to the substantial I_{ds} obtained from the nanowire heterostructures, the $I_{ds} - V_{ds}$ data recorded on undoped GaN nanowire FETs with the same channel length (L_g) (Figure 2a, red line) shows that the nanowire is highly resistive at

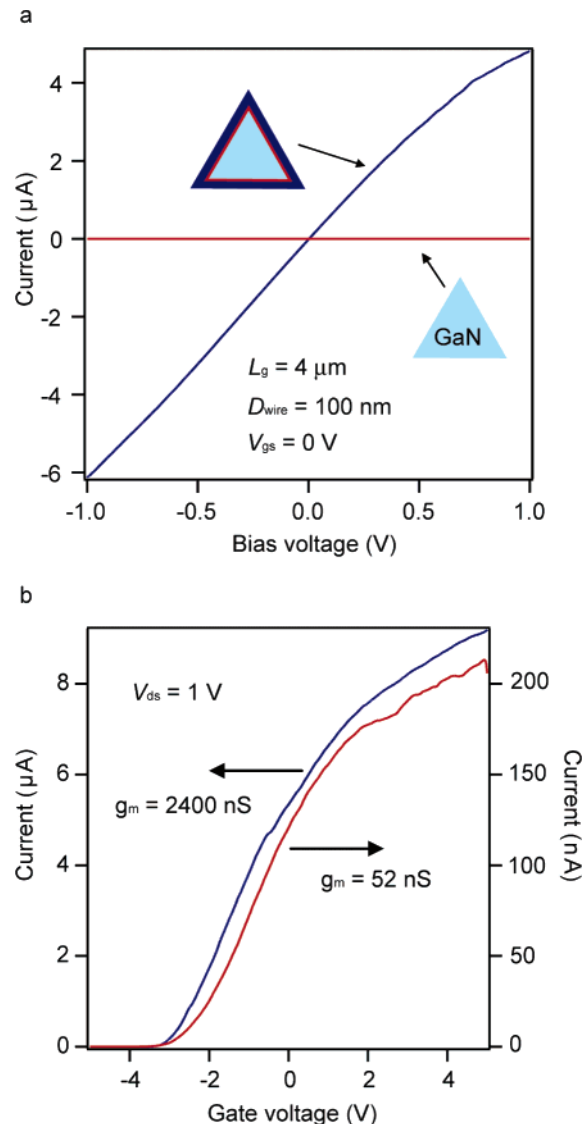


Figure 2. (a) $I_{ds} - V_{ds}$ characteristics recorded on 100-nm-diameter GaN/AlN/Al_{0.25}Ga_{0.75}N (blue) and GaN (red) nanowires with source-drain separation $L_g = 4 \mu\text{m}$ at $V_{gs} = 0$ V. Insets: schematics of the GaN and GaN/AlN/AlGaIn nanowires. (b) $I_{ds} - V_{gs}$ transfer characteristics of the same GaN/AlN/Al_{0.25}Ga_{0.75}N (blue) and GaN (red) nanowires for $V_{ds} = 1$ V.

$V_{gs} = 0$ V, with the total resistance of ca. 8 M Ω . The $I_{ds} - V_{gs}$ data (Figure 2b, red line) further shows that undoped GaN nanowire devices have 50 times smaller conductance and g_m values compared to the GaN/AlN/Al_{0.25}Ga_{0.75}N heterostructures. Because both the GaN/AlN/Al_{0.25}Ga_{0.75}N nanowire heterostructures and the GaN nanowires are undoped, we attribute the large differences in transport properties to the formation of a confined electron gas in the radial nanowire heterostructure through band structure engineering.

Temperature-dependent conductance (G) versus V_{gs} data (Figure 3a) shows that both the on-state G and g_m of the nanowire FET increases as the temperature decreases. This contrasts with the typical behavior in Si-doped n-type GaN nanowire FETs²⁶ as well as that generally observed in doped semiconductors, which show a significant decrease in device on current (I_{on}) at low temperature because charge carriers that come from dopants would freeze-out with decreasing

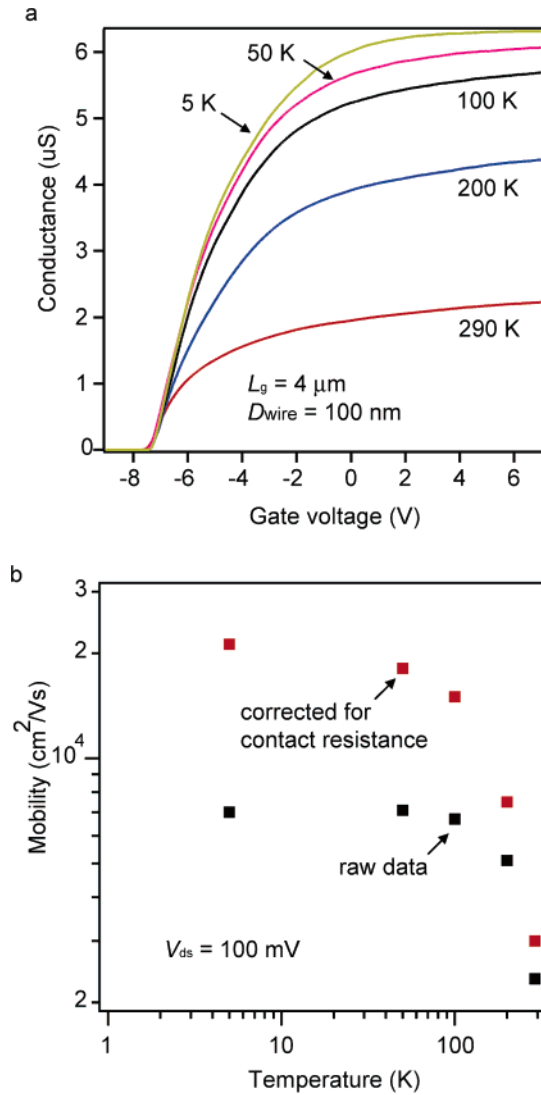


Figure 3. (a) $G - V_{\text{gs}}$ curves recorded at different temperatures for a 100-nm-diameter GaN/AlN/Al_{0.25}Ga_{0.75}N nanowire with $L_g = 4 \mu\text{m}$. $G - V_{\text{gs}}$ curves are slightly offset for clarity. (b) Measured (black symbols) and intrinsic (red symbols) electron mobility of GaN/AlN/Al_{0.25}Ga_{0.75}N nanowire at different temperatures, where the intrinsic values were obtained after the correction for contact resistance.

temperature. The increase in conductance is, however, consistent with and provides strong evidence for an electron gas in these undoped nanowire heterostructures.

In addition, the values of g_m were determined from the analysis of $G - V_{\text{gs}}$ curves at different temperatures (Figure 3a) and then used to estimate the peak electron mobility (μ) using the charge control model,²⁷ $dI/dV_g = g_m = \mu(C_g/L_g^2)V_{\text{ds}}$, where C_g is the gate capacitance²⁸ and $L_g = 4 \mu\text{m}$ is the channel length. The calculated temperature-dependent electron mobility data of the GaN/AlN/Al_{0.25}Ga_{0.75}N nanowire is depicted in Figure 3b. Electron mobilities determined from the raw data first increase drastically as the temperature decreases from room temperature to 100 K, and then begin to saturate at lower temperature. The electron mobility at room-temperature reaches 2300 cm^2/Vs , approaching the best reported electron mobility (2500 cm^2/Vs) in planar GaN/Al_{0.1}Ga_{0.9}N heterostructures grown on bulk GaN substrates,²⁹

and is several times higher than the best value (650 cm^2/Vs) reported in n-type GaN nanowire nanodevices.³ At room temperature, phonon scattering³⁰ is expected to dominate in the single-crystal nanowire heterostructures. As the temperature is decreased from room temperature to 100 K, phonon scattering is reduced significantly, thus explaining the sharp increase in electron mobility. Mobility then starts to saturate at lower temperature due to the suppression of phonon scattering as observed in planar HEMT structures.^{29,30}

To determine the intrinsic mobility of GaN/AlN/Al_{0.25}Ga_{0.75}N nanowires, four-probe transport measurements were also carried out to determine the contact resistance as a function of temperature (Figure S1). The specific source/drain contact resistance determined from these measurements, $2.3 \times 10^{-5} \Omega\text{cm}^2$, is comparable to the value obtained in GaN/AlGaIn planar structures³¹ and is temperature-independent. This source/drain contact resistance is subtracted from the raw device data to obtain the intrinsic transconductance (g_{in}) of the nanowire devices^{4,12} as well as the temperature-dependent intrinsic electron mobility shown in Figure 3b (red symbols). Significantly, this analysis yields a peak nanowire electron mobility of 21 000 cm^2/Vs at 5 K, which is the best value reported in any semiconductor nanowire system. Although this value is still low compared to the record value of 160 000 cm^2/Vs obtained on the GaN/Al_{0.06}Ga_{0.94}N planar heterostructures at 300 mK,³² we believe that the result is quite promising given that this represents the first study of these nanowire heterostructures. In addition, we note that the scaled sheet carrier density for our nanowire heterostructures, $1 \times 10^{12} \text{ cm}^{-2}$, is comparable to the value obtained in GaN/AlGaIn planar heterostructures with similar mobilities.^{29,30} This value was obtained by assuming a uniform distribution of the electron gas on the three facets.³³

We have also explored the potential of GaN/AlN/Al_{0.25}Ga_{0.75}N nanowire heterostructures as high-performance FETs by fabricating devices incorporating a 6-nm-thick high- k ZrO₂ gate dielectric and metal top-gate electrodes (Figure 4a).³⁴ The $I_{\text{ds}} - V_{\text{ds}}$ characteristics recorded on a representative GaN/AlN/Al_{0.25}Ga_{0.75}N nanowire top-gated device (Figure 4b) show typical n-type MOSFET behavior,¹² with current saturation at more positive V_{ds} values. The $I_{\text{ds}} - V_{\text{gs}}$ transfer curve recorded for $V_{\text{ds}} = 1.5 \text{ V}$ (inset, Figure 4c) shows that the nanowire device has a maximum I_{on} and g_m of 50 μA and 42 μS , respectively. To compare these results with planar heterostructure FET devices, we calculated the scaled values of I_{on} and g_m using the total nanowire diameter as the device width. The scaled I_{on} value for a GaN/AlN/Al_{0.25}Ga_{0.75}N nanowire FET is 500 mA/mm, while the scaled g_m is 420 mS/mm, comparable to the best reported value of 450 mS/mm observed in planar GaN/AlGaIn heterostructures.³⁵

In addition, logarithmic plots of the $I_{\text{ds}} - V_{\text{gs}}$ data recorded at different V_{ds} values (Figure 4c) show that the current drops exponentially below the threshold voltage. The rate of this drop, characterized by the subthreshold slope (S), is 68 mV/dec, which is close to the ideal value of $S = (k_B T/e) \ln(10) \approx 60 \text{ mV/dec}$ at room temperature. This result represents a significant improvement in subthreshold slope compare to

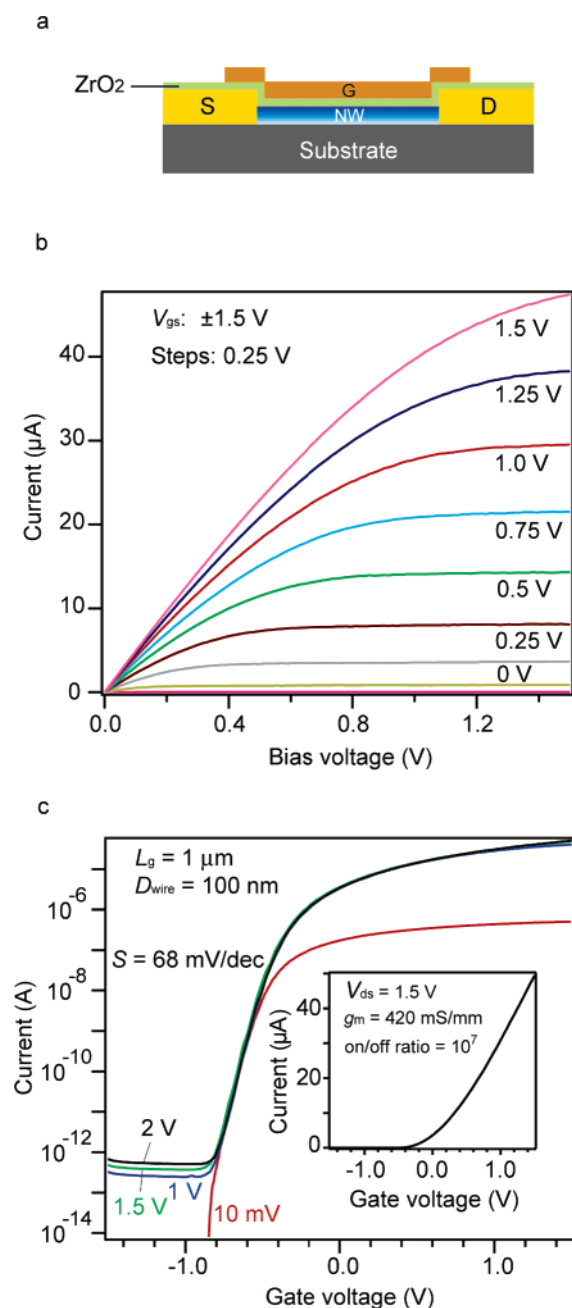


Figure 4. (a) Schematics of top-gate nanowire FET with ZrO_2 insulator layer. (b) $I_{\text{ds}} - V_{\text{ds}}$ data of a 100-nm-diameter $\text{GaN}/\text{AlN}/\text{Al}_{0.25}\text{Ga}_{0.75}\text{N}$ nanowire with $L_{\text{g}} = 1 \mu\text{m}$ at various V_{gs} values (from +1.5 V to -1.5 V, steps are 0.25 V). (c) Logarithmic scale $I_{\text{ds}} - V_{\text{gs}}$ curves recorded at different $V_{\text{ds}} = 2 \text{ V}$, 1.5 V, 1 V, and 10 mV, on the same $\text{GaN}/\text{AlN}/\text{Al}_{0.25}\text{Ga}_{0.75}\text{N}$ nanowire. Inset: linear scale $I_{\text{ds}} - V_{\text{gs}}$ data recorded at $V_{\text{ds}} = 1.5 \text{ V}$.

the best values of 100 mV/dec reported previously in top-gated p-type Ge/Si core/shell nanowire heterostructure FETs¹⁵ and wrap-gated n-type InAs ³⁶ nanowire FETs, and demonstrates the excellent gate coupling and near perfect interface between the $\text{GaN}/\text{AlN}/\text{Al}_{0.25}\text{Ga}_{0.75}\text{N}$ nanowire heterostructure and ZrO_2 dielectric layer. The large maximum on state current, transconductance, and small subthreshold slope also lead to a large on/off current ratio of 10^7 . These results demonstrate the excellent performance of $\text{GaN}/\text{AlN}/\text{Al}_{0.25}\text{Ga}_{0.75}\text{N}$ nanowire heterostructures.

In summary, we have synthesized dislocation-free single-crystal $\text{GaN}/\text{AlN}/\text{Al}_{0.25}\text{Ga}_{0.75}\text{N}$ nanowire heterostructures with well-controlled radial modulation of composition and thickness. Transport measurements on FETs fabricated from undoped $\text{GaN}/\text{AlN}/\text{Al}_{0.25}\text{Ga}_{0.75}\text{N}$ nanowire heterostructures demonstrate the formation of a confined electron gas with high electron mobility and excellent overall device performance. Further improvement of the electrical properties of these new nanowire radial heterostructures might be achieved by optimizing the thickness and composition of AlGaIn shell. These $\text{GaN}/\text{AlN}/\text{Al}_{0.25}\text{Ga}_{0.75}\text{N}$ nanowire HEMTs offer substantial promise as reliable building blocks for nanoscale integrated CMOS electronic circuits, represent a versatile platform for investigating fundamental physics of low-dimensional electron gas systems, and moreover, the chemically inert and robust GaN -based nanowire HEMT devices, which have large surface area and gate sensitivity, could lead to high-sensitivity chemical and biological detectors.³⁷

Acknowledgment. We thank A. J. Garratt-Reed for assistance in EDX elemental mapping measurements. Y.L. acknowledges the Croucher Foundation for postdoctoral fellowship support. C.M.L. thanks the Air Force Office of Scientific Research for support of this work and Thomas-Swan Scientific Equipment Ltd. for support of the MOCVD system. Research at the Oak Ridge National Laboratory SHaRE User Facility was sponsored by the Office of Basic Energy Sciences, U.S. Department of Energy, under contract DE-AC05-00OR22725 with UT-Battelle, LLC.

Supporting Information Available: Temperature-dependent specific contact resistivity data obtained in four-probe transport measurements on $\text{GaN}/\text{AlN}/\text{Al}_{0.25}\text{Ga}_{0.75}\text{N}$ nanowires (Figure S1). This material is available free of charge via the Internet at <http://pubs.acs.org>.

References

- (1) (a) Hu, J.; Odom, T.; Lieber, C. M. *Acc. Chem. Res.* **1999**, *32*, 435. (b) Lieber, C. M. *MRS Bull.* **2003**, *28*, 486.
- (2) (a) Samuelson, L. *Mater. Today* **2003**, *6*, 22. (b) Wang, Z. L. *Mater. Today* **2004**, *7*, 26. (c) Yang, P. *MRS Bull.* **2005**, *30*, 85. (d) Wang, Z. L. *J. Mater. Chem.* **2005**, *15*, 1021.
- (3) Huang, Y.; Duan, X.; Cui, Y.; Lieber, C. M. *Nano Lett.* **2002**, *2*, 101.
- (4) Zheng, G.; Lu, W.; Jin, S.; Lieber, C. M. *Adv. Mater.* **2004**, *16*, 1890.
- (5) Greytak, A. B.; Lauthon, L. J.; Gudiksen, M. S.; Lieber, C. M. *Appl. Phys. Lett.* **2004**, *84*, 4176.
- (6) Cui, Y.; Lieber, C. M. *Science* **2001**, *291*, 851.
- (7) Huang, Y.; Duan, X.; Cui, Y.; Lauthon, L. J.; Kim, K. H.; Lieber, C. M. *Science* **2001**, *294*, 1313.
- (8) (a) Zhong, Z.; Wang, D.; Cui, Y.; Bockrath, M. W.; Lieber, C. M. *Science* **2003**, *302*, 1377. (b) Yang, C.; Zhong, Z.; Lieber, C. M. *Science* **2005**, *310*, 1304.
- (9) Qian, F.; Li, Y.; Gradečak, S.; Wang, D.; Barrelet, C. J.; Lieber, C. M. *Nano Lett.* **2004**, *4*, 1975.
- (10) Qian, F.; Gradečak, S.; Li, Y.; Wen, C. Y.; Lieber, C. M. *Nano Lett.* **2005**, *5*, 2287.
- (11) (a) Erwin, S. C.; Zu, L.; Haftel, M. I.; Efros, A. L.; Kennedy, T. A.; Norris, D. J. *Nature* **2005**, *436*, 91. (b) Shim, M.; Guyot-Sionnest, P. *Nature* **2000**, *407*, 981.
- (12) Shur, M. *Physics of Semiconductor Devices*; Prentice Hall: New Jersey, 1990.
- (13) Lauthon, L. J.; Gudiksen, M. S.; Wang, D.; Lieber, C. M. *Nature* **2002**, *420*, 57.
- (14) Lu, W.; Xiang, J.; Timko, B. P.; Wu, Y.; Lieber, C. M. *Proc. Natl. Acad. Sci. USA* **2005**, *102*, 10046.

- (15) Xiang, J.; Lu, W.; Hu, Y. J.; Wu, Y.; Yan, H.; Lieber, C. M. *Nature* **2006**, *441*, 489.
- (16) Bernardini, F.; Fiorentini, V.; Vanderbilt, D. *Phys. Rev. B* **1997**, *56*, R10024.
- (17) Shen, L.; Heikman, S.; Moran, B.; Coffie, R.; Zhang, N.-Q.; Buttari, D.; Smorchkova, I. P.; Keller, S.; DenBaars, S. P.; Mishra, U. K. *IEEE Electron Device Lett.* **2001**, *22*, 457.
- (18) Sanchez, A. M.; Pacheco, F. J.; Molina, S. I.; Stemmer, J.; Aderhold, J.; Graul, J. J. *Electron Mater.* **2001**, *30*, L17.
- (19) (a) Choi, H. J.; Johnson, J. C.; He, R.; Lee, S. K.; Kim, F.; Pauzauskie, P.; Goldberger, J.; Saykally, R. J.; Yang, P. *J. Phys. Chem. B* **2003**, *107*, 8721. (b) Su, J.; Gherasimova, M.; Cui, G.; Tsukamoto, H.; Han, J.; Onuma, T.; Kurimoto, M.; Chichibu, S. F.; Broadbridge, C.; He, Y.; Nurmikko, A. V. *Appl. Phys. Lett.* **2005**, *87*, 183108.
- (20) Nanowires were synthesized on a c-plane Al_2O_3 substrate in a MOCVD reactor (Thomas Swan Scientific Equipment Ltd.) using trimethylgallium, trimethylaluminum, and ammonia as Ga, Al, and N sources, respectively. We deposited 0.01 M nickel nitrate solution as the nickel nanocluster precursor. GaN cores were grown at 775 °C and sequentially deposited with AlN and AlGaIn shells in hydrogen at 1040 °C.
- (21) Manfra, M. J.; Pfriiffer, L. N.; West, K. W.; Stormer, H. L.; Baldwin, K. W.; Hsu, J. W. P.; Lang, D. V. *Appl. Phys. Lett.* **2000**, *77*, 2888.
- (22) Cross-section TEM samples of GaN/AlN/AlGaIn nanowires were prepared by ultramicrotomy. Nanowires were transferred to Thermanox plastic coverslips and embedded into an Epon-Araldite epoxy resin. Embedded samples were cut perpendicular to the nanowire axis into 70–150-nm-thick slices using a diamond ultramicrotome knife and then transferred onto Cu/lacey-carbon TEM grids. STEM images were collected in a JEOL 22200FS aberration-corrected STEM operated with a 200 kV electron beam and a 100-mrad ADF inner angle. EDX elemental maps were recorded using a VG HB603 STEM.
- (23) Gradečak, S.; Qian, F.; Li, Y.; Park, H. G.; Lieber, C. M. *Appl. Phys. Lett.* **2005**, *87*, 173111.
- (24) Pennycook, S. J.; Boatner, L. A. *Nature* **1988**, *336*, 565.
- (25) For electrical measurements, nanowire FETs were fabricated in standard back-gate geometry and electrical contacts are defined by electron-beam lithography as described previously.^{4–6} Nanowires are gated via the degenerately doped silicon substrate through a $\text{SiO}_2/\text{Si}_3\text{N}_4$ (100/200 nm) dielectric layer. Source–drain contacts were deposited by thermal evaporation of Ti/Al/Ti/Au (20/80/20/30 nm) and annealed in nitrogen at 800 °C for 30 s to achieve ohmic contact.
- (26) Yu, H. Y.; Kang, B. H.; Park, C. W.; Pi, U. H.; Lee, C. J.; Choi, S. Y. *Appl. Phys. A* **2005**, *81*, 245.
- (27) Martel, R.; Schmidt, T.; Shea, H. R.; Hertel, T.; Avouris, Ph. *Appl. Phys. Lett.* **1998**, *73*, 2447.
- (28) The C_g value of the nanowires was estimated using the Quickfield computer program. A 100-nm-diameter nanowire on a degenerately doped Si substrate with $\text{SiO}_2/\text{Si}_3\text{N}_4$ (100/200 nm) dielectric layers in a global back-gate configuration yields a value of ca. 80 aF/ μm .
- (29) Skierbiszewski, C.; Dybko, K.; Knap, W.; Siekacz, M.; Krupczyński, W.; Nowak, G.; Boćkowski, M.; Łusakowski, J.; Wasilewski, Z. R.; Maude, M.; Suski, T.; Porowski, S. *Appl. Phys. Lett.* **2005**, *86*, 102106.
- (30) Henriksen, E. A.; Syed, S.; Ahmadian, Y.; Manfra, M. J.; Baldwin, K. W.; Sargent, A. M.; Molnar, R. J.; Stormer, H. L. *Appl. Phys. Lett.* **2005**, *86*, 252108.
- (31) Fitch, R. C.; Gillespie, J. K.; Moser, N.; Jenkins, T.; Sewell, J.; Via, D.; Crespo, A.; Dabiran, A. M.; Chow, P. P.; Osinsky, A.; La Roche, J. R.; Ren, F.; Pearton, S. J. *Appl. Phys. Lett.* **2004**, *84*, 1495.
- (32) Manfra, M. J.; Baldwin, K. W.; Sargent, A. M.; West, K. W.; Molnar, R. J.; Caissie, J. *Appl. Phys. Lett.* **2004**, *85*, 5394.
- (33) The spontaneous and piezoelectric polarization effect for (0001) and $\{-110-1\}$ facets are not the same, and this may lead to different carrier densities on the three facets of our nanowire heterostructure. It will be interesting to investigate this point in the future.
- (34) Fifty cycles for ZrO_2 deposition using tetrakis(dimethylamino)-zirconium as the precursor were carried out at 110 °C with each cycle consisting of a 1 s water vapor pulse, a 5 s nitrogen purge, a 3 s precursor, and a 5 s nitrogen purge. Top-gate electrodes were defined by e-beam lithography and deposited with metal Ni/Au (100/50 nm) using thermal evaporation. The top-gate metal slightly overlaps with the source and drain.
- (35) Okita, H.; Kaifu, K.; Mita, J.; Yamada, T.; Sano, Y.; Ishikawa, H.; Egawa, T.; Jimbo, T. *Phys. Status Solidi A* **2003**, *200*, 187.
- (36) Wernersson, L.; Bryllert, T.; Lind, E.; Samuelson, L. *Proc. IEEE Int. Electron Devices Meet.* **2005**, Washington, D.C.
- (37) Wang, H. T.; Kang, B. S.; Ren, F.; Fitch, R. C.; Gillespie, J. K.; Moser, N.; Jessen, G.; Jenkins, T.; Dettmer, R.; Via, D.; Crespo, A.; Gila, B. P.; Abernathy, C. R.; Pearton, S. J. *Appl. Phys. Lett.* **2005**, *87*, 172105.

NL060849Z